

# Phased Array Antenna System Development for Radio Astronomy Applications

Stefan J. Wijnholds *Senior Member, IEEE*, Wim A. van Cappellen, Jan Geralt bij de Vaate, Arnold van Ardenne *Senior Member, IEEE*

**Abstract**—Phased array antenna systems are playing an increasingly significant role in the passive, i.e., receive only, radio astronomy application. They provide attractive features such as a large instantaneous field-of-view, multi-beaming capability and rapid response time. In this paper we present an overview of current developments on phased array antenna systems for radio astronomy with an emphasis on the design challenges posed by this application.

**Index Terms**—phased arrays, antenna systems, radio astronomy, Square Kilometre Array

## I. INTRODUCTION

Radio astronomy has a tradition of posing interesting challenges for antenna designers and developers of antenna systems as illustrated by a recent special issue of the IEEE Transactions on Antennas and Propagation [1]. In this context, phased array antenna systems are increasingly becoming a defining technology in current and planned radio astronomical instruments. Phased array antennas provide attractive features such as a large instantaneous field-of-view (sky coverage), multi-beaming capability and rapid response times [2]. Many developments in the radio astronomical community are geared towards the Square Kilometre Array (SKA) [3], a future radio telescope envisaged to be at least an order of magnitude more sensitive than current instruments. In this review, we present an overview of the (envisaged) application of receive-only phased array antennas in current instruments and the SKA while discussing some of the underlying design considerations.

Radio astronomers are searching for extremely weak noise-like signals. Typical flux values for radio astronomical signals lie in the range  $\sim 10^{-32} - 10^{-22}$  W/m<sup>2</sup>/Hz. A telescope with 25-m aperture diameter with 100% aperture efficiency and a bandwidth of 1 MHz thus receives source powers in the range -203 to -103 dBmW. Therefore, sensitivity is a key figure-of-merit for any radio telescope. It is defined as the ratio of the effective area of the antenna system  $A_{\text{eff}}$  over its system temperature  $T_{\text{sys}}$ , i.e., it is measured as  $A_{\text{eff}} / T_{\text{sys}}$ . Providing a large telescope collecting area and a low system temperature are therefore key design drivers for radio astronomical antenna systems.

An important trend in radio astronomy is an increasing focus on the study of the statistics of samples of objects instead of individual objects. As a result, astronomers like to map

out considerable fractions of the visible sky to a certain pre-specified sensitivity limit. This led to survey speed,  $SS$ , as a new figure-of-merit for radio telescopes defined as

$$SS = \left( \frac{A_{\text{eff}}}{T_{\text{sys}}} \right)^2 \times FoV, \quad (1)$$

where  $FoV$  is the instantaneous field-of-view provided by the telescope.

Phased array systems naturally fit in this picture since they can increase their field-of-view by instantaneously forming multiple beams, which can, in principle, cover a full hemisphere. Another advantage of phased array systems over traditional dishes with a single receiver is their ability to rapidly switch beams. This is attractive for study of transient phenomena, since it allows a fast response if the beam needs to be repointed. Phased array antennas can either be used in aperture array (AA) systems, in which the antenna elements are radiating directly towards the sky, or in phased array feed (PAF) systems, in which the phased array antenna samples the electromagnetic (EM) field in the focal plane of a reflector. In Sec. II, we discuss some design considerations for aperture arrays in the radio astronomical context and how these considerations affected the design of the Low Frequency Array (LOFAR) and the aperture array systems envisaged for the SKA. The PAF systems are discussed in a similar fashion in Sec. III.

## II. APERTURE ARRAYS

### A. Regular vs. irregular, dense vs. sparse

One of the main challenges for AA systems in radio astronomy is that three octaves of bandwidth may need to be covered. It therefore seems attractive to use ultra-wideband receiving elements like a log-periodic or a tapered slot antenna. However, the design of an array of such antennas involves a trade-off between cost and performance. In one extreme case, the array is dense at all frequencies. In this case, the antenna spacing is based on the highest operating frequency, which causes strong oversampling of the EM field at the low-frequency end of the operating range. This is clearly not a cost effective solution, but offers a constant effective area over frequency and well behaved performance. The array could also be made sparse for the highest operating frequencies. This will, however, cause reduced performance at those frequencies. A detailed study on the pros and cons of regular and irregular arrays in both the dense and the sparse regime was conducted

The authors are with the Netherlands Institute for Radio Astronomy (ASTRON), P.O. Box 2, NL-7990 AA, Dwingeloo, The Netherlands. Email: wijnholds@astron.nl, cappellen@astron.nl, vaate@astron.nl, ardenne@astron.nl

TABLE I  
CHARACTERISTICS OF REGULAR AND IRREGULAR ARRAYS IN THE DENSE AND SPARSE OPERATING REGIME.

dense and sparse	side lobes	regular	irregular
		lowered by gain taper	lowered by space taper
dense	grating lobes	none	
	receiver temperature	smooth over scan angle and frequency	
	effective area	constant over frequency, smooth over scan angle	
	element patterns	identical for most elements	depend on position
	main beam size	larger than for sparse array with same number of antennas	
sparse	grating lobes	few high ones	many low ones
	receiver temperature	not smooth over scan angle and frequency	smooth over scan angle and frequency
	effective area	steep decrease with wavelength ( $\sim \lambda^2$ )	
		not smooth over scan angle and frequency	smooth over scan angle and frequency
	element patterns	identical for most elements	depend on position
	field of view	smaller than for dense array with same number of elements	

in the design phase of the LOFAR [4] using EM simulations [5]. The results of this study are summarized in Table I.

In the dense regime, both regular and irregular arrays provide complete sampling of the EM field over the aperture. The behavior of both types of arrays is therefore dictated by the characteristics of a filled aperture. In this regime, large regular arrays are usually the most attractive option, since the embedded element patterns of most elements are identical, which facilitates system design and characterization.

Sparse regular arrays have the disadvantage that their effective area may show very sharp changes due to the appearance of grating lobes. Although these features may be smoothed by an appropriate design of the antenna element and receiving network, it is a fundamental feature of regular arrays that is unattractive for radio astronomical applications. As a result, dense arrays are typically chosen when the required operating frequency range spans at most  $\sim 2$  octaves, such that it can be covered with acceptable oversampling at the low-frequency end and by the transition from the dense to the sparse regime at the high-frequency end. For arrays covering a frequency range larger than  $\sim 2$  octaves, an irregular array design is typically chosen with increasing sparsity towards the edge of the array.

LOFAR exploits both options. We discuss the irregular LBA station array and the regular HBA station array in more detail in Secs. II-C and II-D respectively and demonstrate their performance in the transition from the dense to the sparse regime based on actual data. The feasibility of a dense aperture array with a 3:1 frequency range from 500 to 1500 MHz was demonstrated by the Electronic Multi-Beam Radio Astronomy Concept (EMBRACE) [6], which will be discussed in more detail in Sec. II-F.

### B. Design for calibratability

Radio astronomical instruments based on phased array technology can usually be considered as an array of subarrays. The subarrays are called *stations* and can either be aperture array stations or dishes with a phased array feed. This results in a hierarchical system architecture that poses distinct calibration challenges at station and (synthesis) array level [7]. Each level in this system hierarchy needs to be designed in such a way that variations in the instrumental and environmental conditions that are relevant to the performance of that part of the system can be tracked during an observation.

At synthesis array level, this is usually done by self-calibration, i.e., variations in instrumental response and propagation conditions are calibrated during the observation using the brightest sources in the observed scene. This implies that the individual stations should be sensitive enough to observe a sufficient number of potential calibration sources in an average pointing direction on the time scales dictated by those instrumental and environmental changes. This calibratability problem is discussed extensively in [8, 9] and studies on calibratability aspects are still continuing in the context of SKA development [10]. It turns out that they set requirements on design parameters such as station size, aperture efficiency and station sidelobe level, which we will briefly review below. For a more detailed discussion, the reader is referred to [8, 9].

1) *Station size:* At radio frequencies below  $\sim 400$  MHz, the ionosphere causes a propagation delay that varies with scan angle, a *direction dependent effect (DDE)*. At radio frequencies above  $\sim 1$  GHz, DDEs may be introduced by the troposphere. Ionospheric effects recently received significant attention in view of the development of LOFAR [8, 9] and the Murchison Widefield Array (MWA) [11, 12]. An important conclusion from these studies is, that typical ionospheric conditions enforce a calibration update rate of  $\sim 10$  s. More challenging ionospheric conditions require higher update rates that quickly result in infeasible system specifications, so we will have to accept some loss of observing time due to unfavorable observing conditions at the lowest frequencies.

Measurements on such,  $\sim 10$  s, timescales can be regarded as snapshot observations in which the geometry of the array and the observed scene as well as instrumental and environmental parameters are constant. An information theoretic analysis has shown that we can reliably reconstruct DDEs for only about 10 directions per station provided the calibration sources in these directions have sufficient SNR [13]. Since we always have to filter the signals from the brightest sources in the sky detected via the station sidelobes (more on this in Sec. II-B3), we should be able to characterize the DDEs in every snapshot properly using only 3 – 5 calibration sources inside the field-of-view provided by our main beam. If we can detect three sources, we can fit a 2-D plane to describe the DDEs over the station main beam, while detection of five sources allows us to fit a 2-D paraboloid. This implies, that if the station main beam cross-sections at ionospheric height

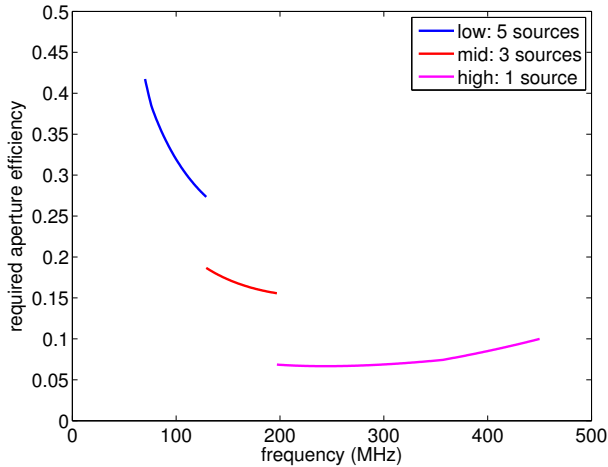


Fig. 1. Required station aperture efficiency for a 98.2-m station as function of frequency when taking the decreasing number of required calibration sources into account.

are non-overlapping, which is the case when the stations are  $\sim 20$  km apart, the station size should be well matched to the typical ionospheric turbulence scales of  $\sim 4^\circ$  at 100 MHz [8]. Assuming a filled aperture, this would imply a minimum station size of 43.4 m. However, a more detailed analysis matching the fitting error to the SNR in a snapshot observation [9] increases this requirement to 57.8 m. At lower frequencies, increasing larger stations are required.

2) *Station aperture efficiency*: The station size requirement was derived based on the assumption that five calibration sources can be found inside the station main beam area. Assuming that a source with an SNR of five in a single 10-s snapshot is sufficiently bright to be used as a calibrator, the combination of main beam size and known statistics on the distribution of astronomical sources over the sky allow us to set a requirement on the sensitivity of a station. Since the station size is already fixed via the main beam size and we usually have a separate requirement on the noise temperature of our receiving system, we can use this information to find the minimum effective area per station such that the aperture efficiency of the station, which is defined as the ratio of the effective area of the station over the physical area of the station, meets a specified minimum value.

Although a full analysis involves many detailed assumptions on, e.g., the noise temperature of the LNA, ionospheric characteristics, tapering of the aperture and observing bandwidth, which is outside the scope of this paper, the general trend over frequency and typical values for the required aperture efficiency are usually similar. Figure 1 shows a typical example that exhibits the following features:

- The required aperture efficiency increases rapidly towards lower frequencies. This is caused by the strong frequency dependence of the sky noise temperature, which dominates the system temperature below  $\sim 300$  MHz and increases more strongly towards lower frequencies than the power spectrum of the calibration sources. This trend needs to be compensated by a higher aperture

efficiency to ensure detection of an appropriate number of calibration sources.

- Since the main beam becomes smaller with increasing frequency while the impact of the ionosphere on the propagation of radio waves becomes smaller as well, we can reduce the number of required calibrators without loss of calibration accuracy towards higher frequencies. This leads to the discontinuities in the plot and to a lower required aperture efficiency.
- At the high frequency end, the system noise is dominated by the noise temperature of the receiver electronics, which was assumed to be 50 K for all frequencies in this analysis. Since the source spectra at these frequencies are such that the source power decreases with frequency, a gradually increasing aperture efficiency is required at the high-frequency end of the frequency range analyzed here.

An important result of this analysis is, that a considerable degree of sparsity is allowed at frequencies between 200 and 400 MHz given the low required aperture efficiency. This makes it feasible to construct cost effective wide-band sparse aperture arrays for radio frequencies below  $\sim 350$  MHz as envisaged for the SKA (see Sec. II-E).

3) *Station sidelobe level*: Since we can deal with only a limited number of source signals in a single snapshot, all except the brightest sources outside the main beam area should be suppressed below the noise level of the snapshot by the sidelobes of the station. If stations have different array configurations or different orientations, one station may have a high sidelobe towards a strong source while another station has a null in the same direction. If the signals from these stations are combined by beamforming or correlation, what matters is not the sidelobe level of each individual station, but the average sidelobe level of all stations [5, 8]. Detailed analysis based on knowledge on the distribution and fluxes of the brightest sources in the sky leads to a requirement on the average station sidelobe level that lies between -40 and -45 dB with respect to the main beam gain. It will be very challenging to achieve such values for each individual station, especially when practical effects like limited station calibration accuracy and element failures are taken into account. This emphasizes the importance of diversity in station orientation or station array configuration across the synthesis array to scramble the station sidelobes and grating lobes.

### C. LOFAR Low Band Antenna

Figure 2 shows an aerial photograph of a Dutch LOFAR station. LOFAR is a phased array radio telescope consisting of 37 stations in The Netherlands and 8 more stations spread across Europe [4]. Each LOFAR station consists of 96 Low Band Antennas (LBAs) and 48 (Dutch stations) or 96 (European stations) High Band Antenna (HBA) tiles each being a  $4 \times 4$  subarray of HBAs whose signals are combined with an analog beamformer. The signals from all LBAs or HBA tiles used during an observation are digitized by 12-bit analog-to-digital converters. The digitized signals are first combined in the station beamformer before the data is sent to the central processing facility in which the beamformed signals of all



Fig. 2. Aerial photograph of a LOFAR station near Exloo (The Netherlands). The station field is about 150 m long and 100 m wide.

stations are further processed. For a more detailed exposition of the LOFAR system, the reader is referred to [4]. In this section, we discuss the LBA array with an emphasis on design considerations. A similar discussion on the HBA array can be found in Sec. II-D.

1) *Antenna design:* The LBA system covers the 10 – 90 MHz frequency range, but its performance is optimized for the 30 – 80 MHz range. The sky noise temperature at 100 MHz is about 1000 K and increases with  $\lambda^{2.55}$  towards lower frequencies where  $\lambda$  denotes the wavelength of the signal. As a result, the overall system noise temperature, which also includes the sky noise temperature, will be dominated by the sky noise temperature. The LOFAR LBAs therefore have a carefully chosen mismatch between the antenna impedance and LNA impedance to turn a simple, easy-to-manufacture, inverted-V-shaped dipole into a broad band antenna system [14]. Use of antenna elements with a relatively low directivity has the additional advantage that it maximizes the sensitivity at low elevations.

The antenna height of 1.70 m is a compromise between high and low frequency performance: if the antenna is higher than about  $3/8 \lambda$ , the antenna will have reduced gain towards broadside at the highest operating frequency. A  $3 \times 3\text{-m}^2$  ground plane consisting of a metal mesh is used to reduce dielectric losses in the ground and to reduce variations in antenna performance due to varying soil conditions, particularly its humidity.

2) *Station configuration design:* The LBAs within a station form an 85-m diameter irregular array with a high density in its center and a low density towards its edge. The minimum distance between the antennas is 2.55 m, enforced by mechanical constraints. This implies that the array becomes sparse at 59 MHz, just above the resonance frequency of the antennas at 57 MHz. The reduction of antenna density with increasing distance from the center of the array apodizes the aperture by a space taper, which reduces the sidelobe level close to the main beam.

Although all stations consist of 96 LBAs, only 48 LBAs

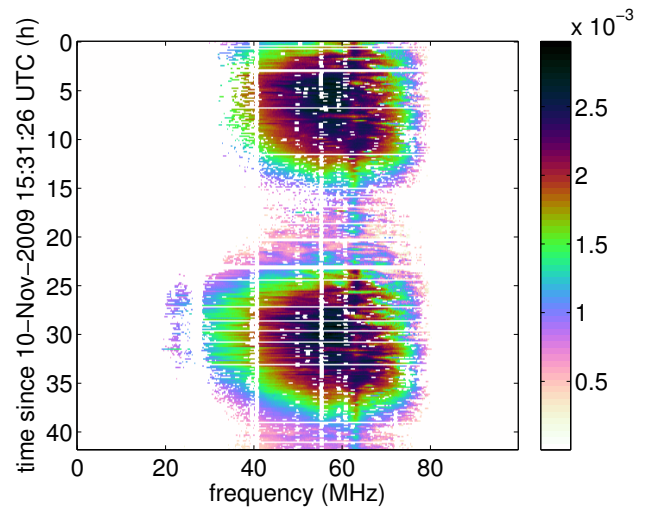


Fig. 3. Contour plot showing the average sensitivity per dipole measured towards calibration source Cas A over a 2-day period for a single 48-antenna station as a function of frequency and time. These results were originally published in [16].

can be active in a Dutch LOFAR station at a given instant in time due to the limited number of receivers. Several antenna selections are defined including an inner array, in which only the elements in the dense center of the array are selected, and an outer array, in which only the 48 outermost antennas are selected. The first configuration provides the densest possible configuration and is therefore most suitable when observing in the upper half of the operational frequency band, while the outer array is most suitable for observations at the low-frequency end. A more detailed description of all configurations can be found in [15].

According to Table I, one of the advantages of irregular arrays over regular arrays is that the effective area does not exhibit sharp features in the array response as function of frequency and pointing direction. This has been verified by in situ measurements of the station sensitivity on Cassiopeia A (Cas A), a strong astronomical source [16]. Cas A never sets on the selected station site in The Netherlands and reaches a lowest elevation of  $22^\circ$  and a highest elevation of  $83^\circ$ . Figure 3 shows the results from a 2-day sensitivity measurement on this source. This plot does not show any sharp features in the average element sensitivity pattern, neither in time (related to the position of Cas A) nor in frequency. It also shows a sharp decrease in sensitivity towards the highest operating frequencies. This result is expected due to the sparseness of the array at these frequencies. The variation of sensitivity over time is the combined result of the station gain towards Cas A at a given instant in time, which is related to the effective area of the station, and the variations in sky noise temperature due to rising and setting of the Galactic plane.

3) *Synthesis array design:* An array of stations or dishes allows radio astronomers to sample an aperture that can potentially be as large as the Earth itself when combining multiple ground based telescopes in so-called Very Long Baseline Interferometry (VLBI). This aperture is sampled by measuring the coherence of the EM field received by

pairs of receiving elements. Astronomers use Earth rotation to obtain more complete sampling of the coherence function over several hours of observation [17, 18].

To obtain as much information about the coherence distribution over the aperture, we want to sample as many different points in the aperture at each instant in time as possible, i.e., we want our stations to form as many distinct *baselines* as possible. A baseline is a vector describing the difference in position between two stations. This desire naturally leads to an array of stations with randomized positions whose density is decreasing exponentially with radius. This principle, in combination with practical constraints on where LOFAR stations could be realized, led to the LOFAR synthesis array configuration.

In Sec. II-B several requirements imposed by calibratability were discussed. As discussed in more detail in [8], the size of the LBA stations is too small to be matched to the scale of typical ionospheric distortions over most of its operational frequency range. At frequencies below  $\sim 40$  MHz, this would require a station size that could be considered unfeasible, but even observations between 40 and 65 MHz may not be successful under typical ionospheric circumstances. This puts a constraint on the observing schedule if long baselines have to be used. If only the inner part of the array is used, the cross-sections of the station main beams will overlap at ionospheric height, which reduces the number of calibration sources per station required to characterize the ionosphere considerably. As a result, also the aperture efficiency requirement can be reduced. Since the longest baselines cannot profit from the vicinity of other stations for ionospheric calibration, the European stations have twice the number of receive paths allowing to process the signals from all 96 LBAs giving them a higher aperture efficiency thereby allowing these stations to find more calibration sources inside their main beam area.

In the LOFAR, the station arrays are rotated copies of each other. This rotation provides effective reduction of the far sidelobe level of the average station beam pattern. As a result, none but the few strongest sources in the sky are detected in individual snapshots outside the main beam area after the station signals are correlated or beamformed in the central processing facility. A more detailed analysis of the scrambling of the sidelobe and grating lobe pattern can be found in [8, 15]. In summary, we can state that the central part of the LOFAR LBA array (up to  $\sim 30$  km) satisfies the calibratability requirements discussed in Sec. II-B, while the full LOFAR LBA array is only calibratable under mild ionospheric conditions.

#### D. LOFAR High Band Antenna

The LOFAR HBA system operates in the 110 – 240 MHz frequency range. Over this range, the sky noise temperature drops from about 800 K to about 100 K, indicating that a proper matching between antenna and LNA is required to ensure that the sky noise temperature remains the dominant component in the system temperature budget. Since the directivity of the individual antennas should be low enough to allow a reasonable scan range, the effective area per element

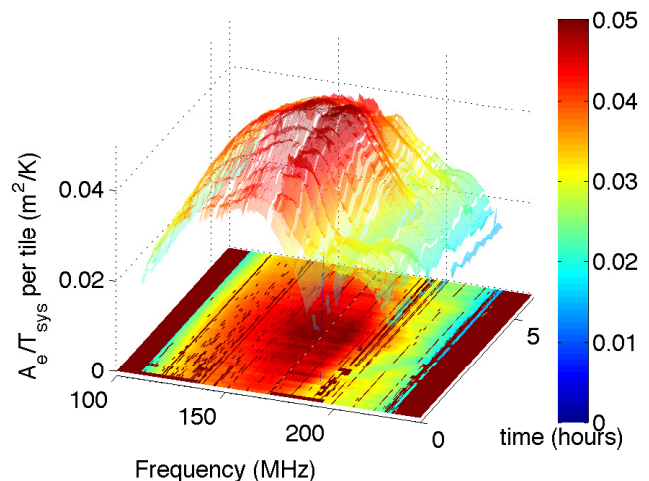


Fig. 4. Sensitivity of a 48-tile HBA station array as function of time around the transit (close to broadside) of the calibration source Cas A and frequency for a single polarization. The plot shows a clear but smooth drop in sensitivity of about 30% that occurs at lower frequencies if Cas A is further away from broadside. This is expected behavior when grating lobes start to appear.

decreases with frequency. As a result, the signals from 16 bow-tie antennas arranged in a  $4 \times 4$  configuration with 1.25-m pitch are combined using an analog beamformer before digitization to ensure a sufficient collecting area per receiver and to keep the costs per unit collecting area reasonable.

Since the HBA system covers only just over an octave of bandwidth, a regular station configuration was chosen that is dense at the low-frequency end and sparse at the high-frequency end. From basic antenna theory, it is known that the appearance of grating lobes can have considerable impact on the directivity of a regular array [19]. When pointed at the zenith, the grating lobes only appear when the observing frequency reaches 240 MHz, but the first grating lobes will appear at increasingly lower frequencies when the array is scanned away from the zenith. This effect was investigated by measuring the sensitivity towards Cas A over a time period starting 3 hours before transit of Cas A close to the zenith and lasting until 3 hours after transit. The results from this measurement are shown in Fig. 4. These measurements clearly show the effect of grating lobes described above at the high frequency part of the plot: the frequency at which the sensitivity starts to drop clearly decreases when Cas A is further away from the zenith. The steep drop in sensitivity towards the lowest frequencies is caused by the combined effect of increasing sky noise temperature and sharp high pass filters to suppress the FM radio signals below 108 MHz.

The filled aperture of the HBA stations easily satisfies the minimum aperture efficiency requirement discussed in Sec. II-B. Also, even the smallest HBA subarrays consisting of only 24 tiles (like the ones shown in Fig. 2) still have a main beam size that is well matched to the scales of typical ionospheric distortions implying that the ionosphere can be properly characterized under normal conditions. Again, the stations throughout the LOFAR have distinct orientations to scramble the grating lobes. This works effectively as demonstrated in

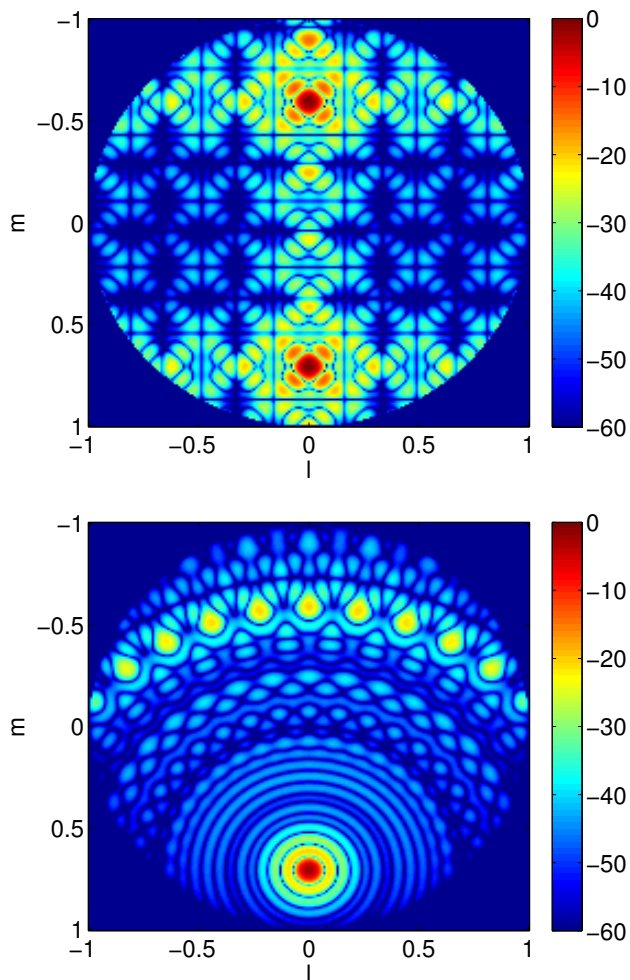


Fig. 5. Average station array factor of nine 24-tile HBA stations with the same orientation (top) and with their orientations homogeneously distributed over 90 degrees (bottom). The color scale represents the power level in dB relative to the main beam peak (previously published in [8, 15]).

Fig. 5.

### E. SKA AA-low

The low frequency aperture array (LFAA) system for SKA is planned to operate in the 50–350 MHz range [20, 21]. It will consist of 1024 stations with a diameter of 35 m spread over a circular area with a diameter of 50 km. Each station is envisaged to consist of 256 receiving elements with an uncooled receiver temperature (including the noise temperature of the LNA) of about 50 K.

In the context of the Aperture Array Verification Programme (AAVP), significant effort was invested in the co-design of a suitable antenna and receiver electronics [22–24]. A suitable antenna should

- have a well behaved antenna impedance over the full frequency range to allow impedance matching to the receiving network;
- not have too high directivity to satisfy the half gain scan range requirement of  $45^\circ$  from broadside;
- have good polarimetric characteristics and



Fig. 6. Low-frequency aperture array prototype antennas installed on the envisaged SKA site in Australia for environmental and electromagnetic testing.

- should be easy to manufacture and deploy in large numbers.

This process resulted in the proposed SKA low-frequency antenna (SKALA) [25], which has a log-periodic structure. Several prototype antennas are currently deployed at sites in Cambridge and in Australia (see Fig. 6) for environmental and electromagnetic testing. At the same time, the design is further optimized for mass production, which is done with care to avoid sacrificing the attractive electromagnetic properties of the original design.

The proposed station size of 35 m does not satisfy the station size requirement discussed in Sec. II-B at its lower operating frequencies. Since both the excess phase introduced by the ionosphere and the main beam size scale linearly with observing wavelength, the minimum station size required depends strongly on the specified reference wavelength. The station size of the SKA AA-low system is therefore still heavily discussed. Motivated by scientific arguments, the current AA-low baseline assumes 35-m stations that should observe down to 50 MHz [20]. As with LOFAR, this may work for the central part of the array where the main beam cross-sections through the ionosphere are overlapping, but is definitely too small to reliably calibrate the full array under typical ionospheric conditions for the lowest frequencies. Also, dividing the total collecting area in many small stations instead of fewer larger stations drives the computing costs up significantly [26]. Ultimately, a trade-off needs to be made between processing costs, observing capabilities and calibratability under various ionospheric conditions.

### F. SKA AA-mid

The aperture array system for the mid-frequencies of the SKA (AA-mid) is envisaged to cover the frequency range from 0.35–1.4 GHz. The main challenges for the AA-mid system are:

- Above  $\sim 300$  MHz, the sky noise temperature is no longer the dominant component of the overall system noise temperature. The noise temperature of the receiving

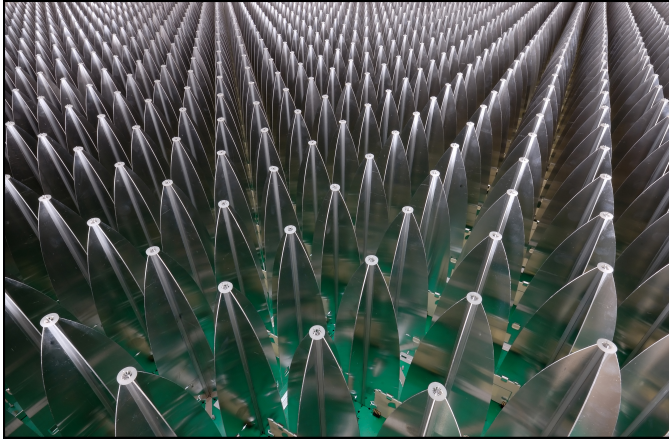


Fig. 7. Picture of an EMBRACE station.

system should therefore be limited to about 50 K over the full operational frequency range. Due to the size of the system, there is no practical, cost-effective way to cool the LNAs, so this low receiving temperature should be achieved with uncooled LNAs behind the antennas. However, micro-cooling may lead to significant reductions in system temperature in future instruments [27].

- SKA receiving systems have a very large collecting area. As a result, the hardware costs for manufacturing and deployment should be well below EUR 1,000.- per square meter. The optimization of the mechanical design should be done without sacrificing performance.
- The AA-mid system will have several tens of antennas per square meter collecting area and will therefore have many analog signal paths and many electronic components. A careful electronic design is necessary to keep energy consumption reasonable.

The potential benefits of an AA-mid system over a dish system are its large instantaneous sky coverage (potentially all-sky), its multi-beaming capability, its observing flexibility and the potential savings in cost for correlation and imaging [26].

In the context of the SKA Design Studies (SKADS) [2, 28], the Electronic Multi-Beam Radio Astronomy Concept (EMBRACE) demonstrator was built. EMBRACE successfully demonstrated the feasibility of a dual polarization aperture array station operating between 500 and 1500 MHz with a system temperature of about 100 K and multi-beaming capability [6], thus providing an excellent starting point for further development and design optimization in the context of AAVP and AIP.

Figure 7 shows a picture of an EMBRACE station. It consists of a regular array of tapered slot or Vivaldi antennas with a 12.5 cm pitch. Tapered slot antennas were chosen for their good performance in an array. The antenna pitch was chosen such that grating lobes will not appear below the highest operating frequency when steering the beams inside the specified scan range of  $45^\circ$  from broadside. As discussed in Sec. II-A, dense regular arrays have a number of attractive features, including a smooth response over scan angle and

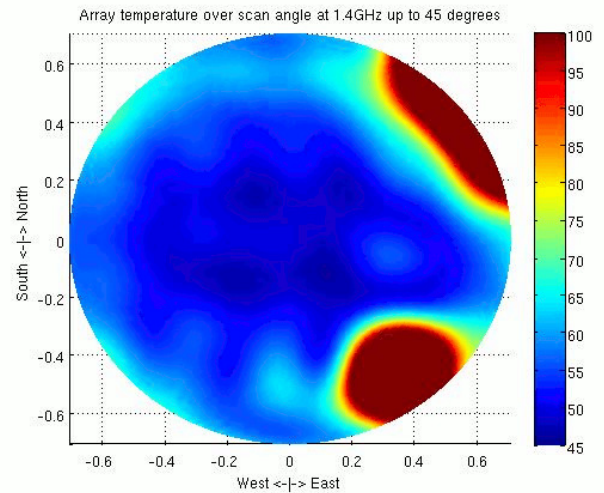


Fig. 8. Measured receiver noise temperature as a function of scan angle of a prototype tile with 121 Vivaldi elements.

frequency and an element response that is constant for most antennas in the array. The latter facilitates the design of a well-matched receiving network, which will be essential to achieve the 50 K noise temperature envisaged for the SKA.

The effect of noise coupling [29-31] plays an important role in a system design that provides the desired low noise temperature over the entire scan range. Figure 8 shows the measured receiver noise temperature of a single tile prototype built in the context of the APERTIF project [32] (see Sec. III-D) indicating that a 50 K system temperature is feasible over a scan range up to  $45^\circ$  from broadside. The hot areas are caused by reflection of the  $\sim 300$  K background from the ground on one of the 25-m dishes at the site of the Westerbork Synthesis radio telescope and by the Sun.

### G. Open issues

The following issues in the area of antenna array research are either still under study or deserve further study:

- *Minimizing the system temperature:* By a combination of further fine-tuning of the impedance match between the antenna and the LNA, further reduction of the LNA noise temperature, new transistor technology and micro-cooling, it may be possible to push the overall system temperature well below 50 K currently assumed for the AA-mid system. This would directly improve the sensitivity of the array.
- *Simple models of mutual coupling:* Full-EM simulations of large irregular arrays are very compute intensive and do not lead to simple models that can be included in calibration routines or used to explore a (part of) design space quickly. For LOFAR, a simple model was developed based on some basic physical principles [15], but this model allows only qualitative exploration. It would be nice to have a simple model that is sufficiently accurate to do a first order quantitative exploration of design space and that is easily parameterized for inclusion in calibration of station arrays.

- *Holistic design optimization:* As we saw in Sec. II-E, optimization of the array configuration involves a trade-off between science requirements, calibratability requirements, computational feasibility and practical constraints. Although much research has been done in the area of beam synthesis, most of that research involves a single array of antennas instead of an array of stations (sub-arrays). Such techniques also focus on optimization of the beam shape without considering the computational costs of processing of the antenna signals. Probably, computational costs can be included as a penalty term in the cost function used for beam synthesis. However, this requires an end-to-end signal processing model, for which a start has been made in [26].
- *Cost reduction:* The SKA will consist of hundreds of thousands of antennas and millions of RF components. We thus face the major challenge to design a high-performance system with low-cost components that are easy to manufacture.

### III. PHASED ARRAY FEEDS

Phased array feeds (PAFs) sample the EM field in the focal plane of a reflector. Therefore, PAFs are always dense regular arrays to ensure that they fully sample the focal spot anywhere in the scan range allowed given the  $f/D$  ratio of the reflector. PAF systems provide a high gain but a limited scan range due to the optics of the reflector. Several instruments using PAF technology are currently being developed, including the Aperture Tile-in-Focus (APERTIF) upgrade of the Westerbork Synthesis Radio Telescope (WSRT) [32], the Australian SKA Pathfinder (ASKAP) [33] and the SKA-survey telescope [20]. These instruments will be briefly discussed in Secs. III-D and III-E. Parallel to the hardware development for these systems, considerable effort was invested in developing optimal beamforming and calibration methods for polarimetric observations with these instruments [34–36]. This work will be reviewed in the next section with an emphasis on its impact on the system design of PAF systems. In Sec. III-B, we discuss the impact of the mounting of the reflector on astronomical observations and in Sec. III-C we discuss design considerations concerning the optics of the reflector system.

#### A. Beamformer optimization

A PAF can be used to form multiple partly overlapping beams on the sky to produce a single large synthesized field-of-view (FoV). Using linear constrained minimum variance (LCMV) beamforming, constraints can be enforced on the shape of these beams. In [34] it is demonstrated that this can be used to reduce the sensitivity ripple over the synthesized FoV from about 35% at the highest frequencies to 12 – 22% over the entire operational frequency range while sacrificing at most 10% of the peak sensitivity. LCMV beamforming can also be used to suppress interfering sources by placing nulls at appropriate locations [37].

An ideal beamformer preserves the polarimetric properties of the impinging EM field, i.e., it compensates for instrumental polarimetric distortions, while providing maximum sensitivity.

If the response of the PAF system to two signals with orthogonal polarization characteristics and the covariance of the noise on the antennas in the absence of an external signal are known for a given scan direction, the optimal beamformer weights can be calculated [35]. Unfortunately, the bright astronomical sources that are used in practice for calibration, are unpolarized. This problem is discussed in [36]. Its main conclusions are:

- PAF systems can be calibrated using an unpolarized source, but this leaves a polarimetric ambiguity that needs to be resolved either by additional measurements on, usually weaker, (partially) polarized sources or by relying on the intrinsic polarimetric quality of the system.
- Many PAF systems consist of two sets of receiving elements, each tuned to a single polarization. In a bi-scalar beamformer, the signals from each set are beamformed separately before the resulting two beamformed signals are combined to get the polarimetrically beamformed output of the full PAF system. This leads to a significantly simpler system design than the full polarimetric beamformer that beamforms both sets simultaneously. With a dipole model and a simulation based on the APERTIF system it is demonstrated that using a bi-scalar beamformer instead of a full polarimetric beamformer sacrifices only a few percent in sensitivity while considerably simplifying the system design. This makes the bi-scalar beamformer the preferred design for the PAF instruments that are currently being developed.
- This all implies that the intrinsic polarimetric quality of the antennas remains a crucial factor despite the development of novel polarimetric calibration methods.

#### B. Reflector mounting

The type of mount is an important consideration when designing a movable reflector for a radio telescope. Fundamentally, there are two types of mount: the altitude-azimuth or  $(alt, az)$ -mount and the equatorial mount [38]. The support structure of an  $(alt, az)$ -mount is usually built on a circular rail track allowing to control the azimuth pointing of the reflector while the altitude or elevation is controlled by tilting the reflector. Mechanically, this is the simplest way to construct the support structure and, hence, many telescopes use this mount, especially the larger ones like the 100-m Effelsberg radio telescope in Germany and the 90-m telescope at Jodrell Bank in the United Kingdom. Unfortunately, an  $(alt, az)$ -mount has two disadvantages:

- 1) The orientation of the principal axes of the reflector and the feed system rotates with respect to the observed field during the observation. This means that, unless the beam pattern of the system has perfect circular symmetry, the beam pattern rotates with respect to the observed field causing gain variations towards sources outside the center of the field-of-view. These gain variations need to be corrected, which complicates processing of the data.
- 2) Two engines have to operate in unison to track a source. This complicates the tracking system.

The first issue poses a trade-off between the mechanical design of the fronted and the complexity of post-processing of the data. Since aperture arrays effectively have a fixed ( $alt, az$ )-mount, they do not only suffer from rotation of the observed field w.r.t. their principal axes, but also from a projection effect due to elevation changes over the observation. The construction of aperture arrays like LOFAR has therefore stimulated research on dealing with time-varying direction dependent effects in radio astronomical observations. This led to a number of novel calibration and imaging algorithms that can deal with these effects.

The two disadvantages of ( $alt, az$ )-mount are solved by the equatorial mount. An equatorial mount has a support structure with one axis of rotation oriented parallel to the rotation axis of the Earth. The orthogonal axis is mounted on the moving part of the support structure and controls the declination. Once the declination is fixed, a source can be tracked by having one engine rotating the reflector at the Earth's angular velocity to compensate the Earth's motion. Since one rotation axis of the telescope is aligned with the rotation axis of the Earth, the principal axes of the reflector and feed remain aligned with the observed field over the entire observation. Depending on geographical location, constructing a reflector with an equatorial mount can be quite challenging from a mechanical point of view. A nice example of a telescope with equatorial mount is the Westerbork Synthesis Radio Telescope (WSRT) in The Netherlands.

### C. Optics design

The ratio of focal length and diameter of a parabolic reflector, the  $f/D$  ratio, is an important characteristic. It has a strong effect on the achievable aperture efficiency and spillover efficiency [19]. Spillover efficiency can have a huge impact on telescope performance since spillover lobes will often be pointed towards the ground, which typically has a temperature of about 290 K, while the sky background temperature is only 3 K in L-band, which is of great astronomical importance. In PAF systems, the  $f/D$  ratio also determines the scan range of the PAF.

Reflectors can be front-fed, having their feed in the prime focus, or have Cassegrain or Gregorian optics using a secondary reflector [19, 38]. Again, each option has its own merits. The prime focus feed has the simplest optics and naturally leads to a symmetric design, which leads to symmetric beam patterns and a simple mechanical design. The disadvantage of a prime focus feed is blockage of the aperture by the feed box and the struts required to support the feed box. This can become particularly troublesome if multiple feeds need to be placed in the feed box to allow reasonably fast switching between observing bands. Therefore, dish designers are currently looking into offset Gregorian optics for the SKA [20] and the expanded Karoo Array Telescope (MeerKAT) in South-Africa [39, 40]. Offset Gregorian optics have the advantage that the view of the primary reflector is not blocked by either the feed box or the secondary reflector and that the feed box can be mounted close to the support structure thus allowing for more space to accommodate multiple feeds. The



Fig. 9. Photograph of the APERTIF prototype system mounted on one of the WSRT dishes.

disadvantages of offset Gregorian systems are their inherent asymmetry, which will cause asymmetries in the side lobe pattern and may even cause some asymmetries in the main beam and the size of the secondary mirror, especially if PAFs are used to form multiple beams.

### D. APERTIF

The goal of the Aperture Tile-in-Focus (APERTIF) project is to increase the survey speed of the Westerbork Synthesis Radio Telescope (WSRT) in The Netherlands [32]. Since APERTIF is an upgrade for an existing radio telescope, specific boundary conditions like the size of the reflector (25 m), the  $f/D$  ratio (0.35) and limits to the size and weight of the feed box are set. An attractive feature of the WSRT is, that it consists of equatorially mounted reflectors. Ultimately, 12 out of 14 WSRT dishes will be equipped with a PAF. These PAFs will operate in the 1130 – 1750 MHz frequency range, will have a system temperature of 70 K and will be capable of providing 37 dual polarized beams. This enhances the instantaneous field-of-view at the important neutral hydrogen frequency of 1.4 GHz to 8 square degrees. Combined with an aperture efficiency of 75% this would improve the survey speed of the WSRT by a factor  $\sim 17$ .

A prototype system has been installed on one of the WSRT dishes and is shown in Fig. 9. It consists of 121 Vivaldi elements arranged in a rectangular grid along two orthogonal orientations to sample the polarimetric properties of the focal field. Holographic measurements were done to study the behavior of the prototype system. In a holographic measurement, a reference telescope (another WSRT dish with a reference feed) is tracking the same source as the telescope-under-test (TUT). By correlating the signals from the reference telescope and the TUT, we can infer information on the far field radiation patterns (in voltage domain) of each of the antenna elements in the PAF on the TUT. These data were used to validate the design of the system and to demonstrate the ability of a PAF system to do the same polarimetric observations as a regular horn feed [41]. These measurements also confirmed the results

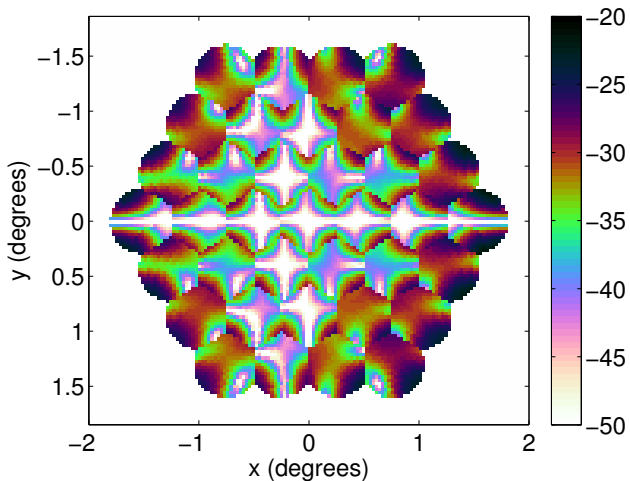


Fig. 10. Inverse XPD for one direction of linear polarization for a simulated APERTIF system at 1.4 GHz over its full instantaneous FoV formed by 37 beams (originally published in [36]).

obtained from the simulations developed for the studies on calibration and beamforming discussed in Sec. III-A.

Most practically feasible calibration and beamforming schemes optimize the response in the main beam centers of each of the PAFs beams. The polarimetric behavior over the FoV has therefore been a primary concern. Figure 10 shows simulation results for the inverse of the Cross-Polarization Discrimination (XPD, hence the negative dB scale) for one direction of linear polarization when using bi-scalar beamforming and relying on the intrinsic polarimetric quality of the Vivaldi elements. The results indicate that a PAF system for the WSRT can potentially achieve an XPD better than 20 dB over its entire FoV and even higher values for its central beams. The simulations show an asymmetric pattern. This is caused by the asymmetries in the design of the pick-up lines feeding the antennas.

#### E. ASKAP and the SKA survey telescope

The Australian SKA Pathfinder (ASKAP) is a survey telescope that will ultimately consist of 36 prime focus-fed 12-m parabolic reflectors [33, 42]. It is currently being built in the Murchison Radio-astronomy Observatory in the Western Australian desert. The ASKAP dishes are spread over an area with 6-km diameter with the highest density of dishes near the center of the array.

In principle, high  $f/D$  values ( $>0.6$ ) allow better performance with a phased array feed, but are mechanically hard to realize. However, low  $f/D$  values ( $<0.45$ ) lead to under-illumination of the dish. This trade-off resulted in  $f/D = 0.5$  [33]. The dishes are mounted using an  $(alt, az)$ -mount, which causes their radiation pattern to rotate w.r.t. the observed field over an observation. Although it has been considered to compensate this effect electronically in the beamformer of the phased array feed, the ASKAP provides a third axis that can rotate the feed box and its support structure around the optical axis of the dish, thereby allowing to compensate this effect mechanically [33].

The reflector dishes are front-fed with a "checkerboard" array optimized for the 700 – 1800 MHz range [43, 44]. The checkerboard array consists of square conducting patches on an electrically thin dielectric sheet. This allows easy manufacturing by printing the patch antennas on a printed circuit board (PCB). The PCB is separated from the ground plane by a foam layer. The opposite corners of each square are connected to a differential LNA by transmission lines through the foam layer and the ground plane.

ASKAP is a precursor to the SKA and is envisaged to become an integral part of the SKA survey telescope [20]. That system is envisaged to consist of the original 36 ASKAP dishes augmented with 60 15-m SKA dishes. The SKA survey telescope will have a maximum baseline of 100 km and will ultimately cover the 350 – 4000 MHz range using three distinct feed systems covering 350 – 900 MHz, 650 – 1670 MHz and 1500 – 4000 MHz respectively. The second feed system will be installed first and matches the ASKAP range pretty well. The other two feed systems will only be installed during the second phase of the SKA.

The SKA reflectors are envisaged to have offset-Gregorian optics to provide a clean aperture and allow for a large feed box providing space for multiple PAFs for different frequency bands. These reflectors will have an  $(alt, az)$  mount, but a third axis of rotation is not foreseen. This implies that the rotation of the feed w.r.t. the observed field needs to be compensated for in the PAF beamformer or in post-processing. The availability of the third axis in ASKAP makes that precursor an excellent test bed to develop and validate the required signal processing technologies by repeated observations on the same fields with and without mechanical compensation by rotation of the feed box.

#### IV. CONCLUDING REMARKS

Phased array technology can enhance the capabilities of radio telescopes by providing a large instantaneous sky coverage, multi-beaming capability and more observing flexibility. In this paper, we presented an overview of developments of phased array systems for radio astronomy, both for aperture arrays and for phased array feed systems. We discussed the design challenges caused by the conflicting demands of the application. The desire to measure increasingly weaker signals requires a high sensitivity and high mechanical and electronic stability.

A high sensitivity requires a cost effective way to build a large collecting area. A cost-effective telescope design will involve a choice for appropriate limits on stability and manufacturing tolerances. As a result, the instrument must have self-calibration capability, which is also required to deal with varying ionospheric and tropospheric conditions during the observation. The telescope will therefore have to be designed for calibratability. We have illustrated the impact of this requirement for aperture arrays, showing that it leads to requirements on station size, station aperture efficiency and station sidelobe level, which are very valuable input for the design of the station antenna array.

A high sensitivity also requires a low receiver temperature, which, together with the desired mechanical and electronic

stability, drives the costs upwards. The computational demands to process data from many small receivers also comes at a cost. Ultimately, this does not only ask for technological advances like micro-cooled low-noise amplifiers and optimization of antenna design for manufacturability, but for a holistic design approach of the complete system to make appropriate trade-offs between all subsystems involved from antenna design to data processing.

## REFERENCES

- [1] K. F. Warnick, M. V. Ivashina and S. G. Hay (eds), "Special Issue on Antennas for Next Generation Radio Telescopes," *IEEE Transactions on Antennas and Propagation*, **AP-59**, 6, June 2011.
- [2] A. van Ardenne, J. D. Bregman, W. A. van Cappellen, G. W. Kant and J. G. bij de Vaate, "Extending the Field of View with Phased Array Techniques: Results of European SKA Research," *Proceedings of the IEEE*, **97**, 8, August 2009, pp. 1531-1542.
- [3] P. E. Dewdney, P. J. Hall, R. T. Schilizzi and T. J. L. W. Lazio, "The Square Kilometre Array," *Proceedings of the IEEE*, **97**, 8, August 2009, pp. 1482-1496.
- [4] M. P. van Haarlem et al., "LOFAR: The Low-Frequency Array," *Astronomy & Astrophysics*, **556**, A2, August 2013.
- [5] W. A. van Cappellen, S. J. Wijnholds and J. D. Bregman, "Sparse Antenna Array Configurations in Large Aperture Synthesis Radio Telescopes," 3rd European Radar Conference (EuRAD), Manchester, United Kingdom, 13-15 September 2006, pp. 76-79.
- [6] G. W. Kant, P. D. Patel, S. J. Wijnholds, M. Ruiter and E. van der Wal, "EMBRACE: A Multi-Beam 20,000-Element Radio Astronomical Phased Array Antenna Demonstrator," *IEEE Transactions on Antennas and Propagation*, **AP-59**, 6, June 2011, pp. 1990-2003.
- [7] S. J. Wijnholds, S. van der Tol, R. Nijboer and A. J. van der Veen, "Calibration Challenges for Future Radio Telescopes," *IEEE Signal Processing Magazine*, **27**, 1, January 2010, pp. 30-42.
- [8] S. J. Wijnholds, J. D. Bregman and A. van Ardenne, "Calibratability and its Impact on Configuration Design for the LOFAR and SKA Phased Array Radio Telescopes," *Radio Science*, **46**, RS0F07, 8 November 2011.
- [9] J. D. Bregman, "System Design and Wide-field Imaging Aspects of Synthesis Arrays with Phased Array Stations," *Ph.D. Thesis*, University of Groningen, Groningen, The Netherlands, 14 December 2012.
- [10] O. Smirnov, "Ghosts, Surprises & Simulations: Performance Limits of Future Instruments," IEEE AfriCon / URSI BEJ track, Port Louis, Mauritius, 9-12 September 2013.
- [11] D. A. Mitchell et al., "Real-time Calibration of the Murchison Widefield Array," *IEEE Journal of Selected Topics in Signal Processing*, **2**, 5, October 2008, pp. 707-717.
- [12] C. J. Lonsdale, D. Oberoi, A. J. Coster and P. J. Erickson, "The Effects of Variable Ionospheric and Plasmaspheric Faraday Rotation on Low Frequency Radio Arrays," XXXth General Assembly and Scientific Symposium of the International Union of Radio Science (URSI GASS), Istanbul, Turkey, 13-20 August 2011.
- [13] S. van der Tol, B. D. Jeffs and A. J. van der Veen, "Self-calibration for the LOFAR Radio Astronomical Array," *IEEE Transactions on Signal Processing*, **55**, 9, September 2007, pp. 4497-4510.
- [14] S. W. Ellingson, "Antennas for the Next Generation of Low-Frequency Radio Telescopes," *IEEE Transactions on Antennas and Propagation*, **AP-53**, 8, August 2005, pp. 2480-2489.
- [15] S. J. Wijnholds, "LOFAR Configuration Considerations as a Design Exercise for the SKA," SKA Memo 143, SKA Project Office, Manchester, United Kingdom, July 2012.
- [16] S. J. Wijnholds and W. A. van Cappellen, "In Situ Antenna Performance Evaluation of the LOFAR Phased Array Radio Telescope," *IEEE Transactions on Antennas and Propagation*, **AP-59**, 6, June 2011, pp. 1981-1989.
- [17] R. A. Perley, F. R. Schwab and A. H. Bridle, "Synthesis Imaging in Radio Astronomy," *Astronomical Society of the Pacific Conference Series*, **6**, BookCrafters Inc., 1994.
- [18] A. R. Thompson, J. M. Moran and G. W. Swenson, "Interferometry and Synthesis in Radio Astronomy," Krieger Publishing Company, Malabar, Florida, 1998.
- [19] C. A. Balanis, "Antenna Theory - Analysis and Design," 2nd edition, John Wiley & Sons, 1997.
- [20] P. E. Dewdney et al., "SKA1 System Baseline Design," SKA Project Office, Manchester, United Kingdom, Tech. Report SKA-TEL-SKO-DD-001, 12 March 2013.
- [21] R. McCool and T. J. Cornwell, "Miscellaneous Corrections to the Baseline Design", SKA Project Office, Manchester, United Kingdom, Tech. Report SKA-TEL-SKO-DD-003, 27 October 2013.
- [22] E. de Lera Acedo, "SKA AA-low: LPD Antenna (SKALA) & Path Towards AAVS0 at Cambridge," Aperture Array Verification Programme (AAVP) Workshop, Dwingeloo, The Netherlands, 12-16 December 2011.
- [23] G. Vironne et al., "AAVS0 Results, Dual Polarized Vivaldi Antenna," Aperture Array Verification Programme (AAVP) Workshop, Dwingeloo, The Netherlands, 12-16 December 2011.
- [24] F. Perini, "AAVS Receiver," Aperture Array Verification Programme (AAVP) Workshop, Dwingeloo, The Netherlands, 12-16 December 2011.
- [25] E. de Lera Acedo, "SKALA: A Log-Periodic Antenna for the SKA," International Conference on Electromagnetics in Advanced Applications (ICEAA), Cape Town, South Africa, 2-7 September 2012, pp. 353-356.
- [26] S. J. Wijnholds and R. Jongerius, "Computing Cost of Sensitivity and Survey Speed for Aperture Array and Phased Array Feed Systems," IEEE AfriCon / URSI BEJ track, Port Louis, Mauritius, 9-12 September 2013.
- [27] H. S. Cao, R. H. Witvers, S. Vanapalli, H. J. Holland and H. J. M. ter Brake, "Cooling a Low Noise Amplifier with a Micromachined Cryogenic Cooler," *Review of Scientific Instruments*, **84**, 105102, October 2013.
- [28] S. A. Torchinsky, A. van Ardenne, T. van den Brink, A. J. J. van Es and A. J. Faulkner (eds.), "Wide Field Science and Technology for the Square Kilometre Array - Proceedings of the SKADS Conference", Château de Limelette, Belgium, 3-6 November 2009.
- [29] R. Maaskant and E. E. M. Woestenburg, "Applying the Active Antenna Impedance to Achieve Noise Match in Receiving Array Antennas," IEEE International Symposium on Antennas and Propagation, Hawaii, United States, 10-15 June 2007, pp. 5889-5892.
- [30] M. V. Ivashina, R. Maaskant and B. Woestenburg, "Equivalent System Representation to Model the Beam Sensitivity of Receiving Antenna Arrays," *IEEE Antennas and Wireless Propagation Letters*, **7**, 2008, pp. 733-737.
- [31] K. F. Warnick, E. E. M. Woestenburg, L. Belostotski and P. Russer, "Minimizing the Noise Penalty Due to Mutual Coupling for a Receiving Array," *IEEE Transactions on Antennas and Propagation*, **AP-57**, 6, June 2009, pp. 1634-1644.
- [32] W. A. van Cappellen and L. Bakker, "APERTIF: Phased Array Feeds for the Westerbork Synthesis Radio Telescope," IEEE International Symposium on Phased Array Systems and Technology, 12-15 October 2010, pp. 640-647.
- [33] D. R. DeBoer et al., "Australian SKA Pathfinder: A High-Dynamic Range Wide-Field of View Survey Telescope," *Proceedings of the IEEE*, **97**, 8, August 2009, pp. 1507-1521.
- [34] M. V. Ivashina et al., "An Optimal Beamforming Strategy for Wide-Field Surveys with Phased-Array-Fed Reflector Antennas," *IEEE Transactions on Antennas and Propagation*, **AP-59**, 6, June 2011, pp. 2058-2065.
- [35] K. F. Warnick, M. V. Ivashina, S. J. Wijnholds and R. Maaskant, "Polarimetry With Phased Array Antennas: Theoretical Framework and Definitions," *IEEE Transactions on Antennas and Propagation*, **AP-60**, 1, January 2012, pp. 184-196.
- [36] S. J. Wijnholds, M. V. Ivashina, R. Maaskant and K. F. Warnick, "Polarimetry With Phased Array Antennas: Sensitivity and Polarimetric Performance Using Unpolarized Sources for Calibration," *IEEE Transactions on Antennas and Propagation*, **AP-60**, 10, October 2012, pp. 4688-4698.
- [37] B. D. Jeffs et al., "Signal Processing for Phased Array Feeds in Radio Astronomical Telescopes," *IEEE Journal of Selected Topics in Signal Processing*, **2**, 5, October 2008, pp. 635-646.
- [38] J. D. Kraus, "Radio Astronomy," 2nd edition, Cygnus-Quasar Books, 1986.
- [39] J. L. Jonas, "MeerKAT - The South African Array with Composite Dishes and Wide-Band Single Pixel Feeds," *Proceedings of the IEEE*, **97**, 8, August 2009, pp. 1522-1530.
- [40] D. B. Davidson, "Potential Technological Spin-offs from MeerKAT and the South African Square Kilometre Array Bid," *South African Journal of Science*, **108**, 1050, 2012, pp1-3.
- [41] W. A. van Cappellen and S. J. Wijnholds, "Polarimetric Calibration Results of an APERTIF Phased Array Feed," International Conference on Electromagnetics in Advanced Applications (ICEAA), September 2012, pp. 698-701.
- [42] A. Chippendale and A. Schinckel, "ASKAP: Progress Towards 36 Parabolic Reflectors with Phased Array Feeds," XXXth General Assembly and Scientific Symposium of the International Union of Radio Science (URSI GASS), Istanbul, Turkey, 13-20 August 2011.

- [43] S. G. Hay et al., "Focal Plane Array Development for ASKAP (Australian SKA Pathfinder)," Second European Conference on Antennas and Propagation (EuCAP), Edinburgh, United Kingdom, 11-16 December 2007.
- [44] S. G. Hay, "Comparison of Single-ended and Differential Beamforming on the Efficiency of a Checkerboard Phased Array Feed in Offset- and Front-Fed Reflectors," Fourth European Conference on Antennas and Propagation (EuCAP), Barcelona, Spain, 12-16 April 2010.

PLACE  
PHOTO  
HERE

**Stefan J. Wijnholds** (S'06-M'10-SM'12) was born in The Netherlands in 1978. He received the M.Sc. degree in astronomy and the M.Eng. degree in applied physics (both cum laude) from the University of Groningen, The Netherlands, in 2003, and the Ph.D. degree (cum laude) from Delft University of Technology, Delft, The Netherlands, in 2010.

After his graduation in 2003, he joined the R&D Department of ASTRON, the Netherlands Institute for Radio Astronomy, Dwingeloo, The Netherlands, where he works with the system design and integra-

tion group on the development of the next generation of radio telescopes. From 2006 to 2010, he was also affiliated with the Delft University of Technology, Delft, The Netherlands. His research interests lie in the area of array signal processing, specifically calibration and imaging, and system design of the next generation of radio telescopes.

PLACE  
PHOTO  
HERE

**Wim A. van Cappellen** obtained his M.Eng. degree (cum laude) in electrical engineering from Delft University of Technology, The Netherlands, in 1998. From 1998 to 2001 he held a position at Thales Nederland B.V. to study innovative concepts for naval radar systems. Since 2001, he is with the Netherlands Institute for Radio Astronomy (ASTRON) where he is now responsible for the antenna and RF research and development. His research interests are ultra wideband antenna arrays and phased array feeds for application in radio-astronomical low-noise

receiving systems. He is currently leading the phased array feed project APERTIF.

PLACE  
PHOTO  
HERE

**Jan Geralt bij de Vaate** received his M.Eng. degree in electrical engineering from the Twente University, the Netherlands, in 1988. He joined Thales where he worked on microwave modules for naval phased array systems and in particular on monolithic microwave integrated circuits. In 1997 he switched to Nokia Research Center, Helsinki, Finland, to work as a project leader on handset integration. In 1998 he became scientific project manager at ASTRON, the Netherlands Institute for Radio Astronomy. Besides being responsible for the initiation of an integrated

circuits group, he has been project manager of aperture array demonstrator and phased array feed projects. Mr. Bij de Vaate is currently the Square Kilometre Array technology manager at ASTRON. He is appointed leader of the international consortium for the design of the aperture array systems of the SKA. His research interests are low noise active antennas on which topic he authored and co-authored 60 conference and journal papers.

PLACE  
PHOTO  
HERE

**Arnold van Ardenne** (SM'10) holds a degree in Electrical Engineering and Technical Physics from Twente University in the Netherlands. He worked as Researcher on Phased Array Radar at TNO defense laboratory in the field of electromagnetic modeling and development of phase shifters. He joined ASTRON's technical staff as scientific project manager in the development of low noise feeds and receivers, systems for Very Long Baseline Interferometry and subsequently on the development of superconducting (sub)mm broadband focal plane array receivers

for ground and space applications, the latter at the initial stage of the later ESA cornerstone satellite mission Herschel.

In 1990, he became responsible for new systems development as Business units manager R&D at Ericsson Radio Systems. In 1994 he rejoined ASTRON as Director R&D to develop and implement the organizational and managerial framework for an advanced instrumentation and technology program in the Radio and Optical/IR, in particular for the rejuvenation of the Westerbork Aperture Synthesis Array, preparing the way for the next generation radio telescopes (LOFAR and SKA), optical instruments for major observatories on ESOs telescopes in Chili, La Palma, and participation in the mid IR-instrument for the James Webb Space Telescope. He became responsible for developments for the SKA, coordinating the European design study based on phased arrays and other new instruments related to performance monitoring elements for the European GNSS system Galileo and remains involved in ASTRON's SKA program.

Arnold van Ardenne has been chairing and member of many (inter)national committees, advisory and refereeing panels related to technology, science, instrumentation and management and the diffusion of technologies in the public and market sector authoring numerous articles. He is a long standing member of the IEEE, Dutch Society of Electronic and Radio Engineers in the Netherlands and is president of the Dutch national URSI committee. He is an adjunct Professor in Radio Astronomy at Chalmers University of Technology in Gothenburg, Sweden and involved in the Swedish SKA program.